

Low-temperature anomalous specific heat without tunneling modes: a simulation for a-Si with voids

Serge M. Nakhmanson and D. A. Drabold

Department of Physics and Astronomy, Condensed Matter and Surface Science Program, Ohio University, Athens, Ohio 45701-2979

(January 2, 2018)

Using empirical potential molecular dynamics we compute dynamical matrix eigenvalues and eigenvectors for a 4096 atom model of amorphous silicon and a set of models with voids of different size based on it. This information is then employed to study the localization properties of the low-energy vibrational states, calculate the specific heat $C(T)$ and examine the low-temperature properties of our models usually attributed to the presence of tunneling states in amorphous silicon. The results of our calculations for $C(T)$ and “excess specific heat bulge” in the $C(T)/T^3$ vs. T graph for *voidless* a-Si appear to be in good agreement with experiment; moreover our investigation shows that the presence of localized low-energy excitations in the vibrational spectrum of our models *with voids* strongly manifests itself as a sharp peak in $C(T)/T^3$ dependence at $T < 3K$. To our knowledge this is the first numerical simulation that provides adequate agreement with experiment for the very low-temperature properties of specific heat in disordered systems *within* the limits of harmonic approximation.

I. INTRODUCTION

The main goal of the computational project presented below was to construct a set of realistic models for device quality a-Si (a-Si:H) material, containing nanovoids in the structure, and explore the vibrational properties of these models, especially the localization patterns of the low-energy states that emerge after introducing a void into silicon continuous random network (CRN). Modern computational facilities allow us to study models of up to several hundreds of atoms with *ab initio* methods and thousands of atoms if we switch to empirical techniques, which is especially helpful for realistic large scale modeling of amorphous materials. We can perform simulated quenching and annealing for these models, looking for their most energetically favorable geometry, then we can calculate the dynamical matrices for our systems and diagonalize them exactly, receiving their eigenvalues together with the conjugate eigenvectors. This data gives us the ability to construct the vibrational density of states (VDOS) for a given model as well as to look at the localization properties of individual eigenstates of its dynamical matrix. The calculation of specific heat can be seen as a natural extension of these techniques because we can do it with a little effort once we have obtained

the VDOS information for the model.

In Section II of this paper we present the details of our model construction scheme for a large (based on 4096 atom model) family of models for a-Si with voids and introduce a set of methods we employ for geometry optimization, dynamical matrix and specific heat calculations. In Section III we discuss the results of our calculations of vibrational properties and specific heat for the models considered and finally in Section IV we summarize our findings about the influence of localized low-energy vibrational modes on the thermodynamical properties of amorphous silicon.

II. MODEL CONSTRUCTION AND COMPUTATIONAL PROCEDURES

We use the Djordjevic, Thorpe and Wooten 4096 atom model¹ for a-Si (referred to as DTW in what follows) constructed with the Wooten, Winer and Weaire bond switching algorithm² as a base for building a family of models with voids. The length of the side of a cubic supercell for this model is approximately 43 Å. As our first step we optimize the geometry of the basic model which results only in minor network rearrangements; this relaxed geometry is then used for producing all of the following models with voids. To cut out a void we pick an arbitrary atom in the network and remove it as well as the consecutive spherical shells of its neighbors. We find that our results do not depend much on which atom we select for this procedure.

By applying this procedure we have built three models with voids of different diameter: a 4091 atom model with a “small void” (only one atom and four of its nearest neighbors removed) — a void of approximately 5 Å in diameter, 4069 atom “medium void” model with 10 Å void and 4008 atom “large void” model with 15 Å void. We refrained from building models with even larger voids to prevent possible interaction of a void with its own “ghost” images in the neighboring periodically translated supercells.

Every model with voids was then quenched to minimize the forces acting on atoms in the network. The atomic forces must be small for the application of the harmonic approximation for the total energy of the system, which is required for the dynamical matrix calculation. After the dynamical matrix calculation for every model mentioned above, the eigenvalue and eigenvector data was

used to produce VDOS and inverse participation ratio³ (IPR) graphs for the model, calculate its specific heat and visualize the spatial localization/delocalization characteristics of some of its vibrational modes (the ones which behavior we found most interesting).

For geometry optimization of the models (simulated quenching) and dynamical matrix calculation we employ a molecular dynamics code “Estrelle” developed by the authors of this paper. The code is built around an empirical environment-dependent interatomic potential (EDIP), which has been recently introduced by Bazant and Kaxiras^{4–6}. In general, this potential inherits the well established Stillinger-Weber⁷ format for two- and three-body interactions, but now these interaction terms depend on the local atomic environment through an effective coordination parameter. Our testing results for EDIP and its performance in comparison to our previous *ab initio* calculations⁸ are described elsewhere⁹.

The force tolerance threshold in simulated quenching mode of our MD program is set to be 0.01 eV/Å for all its applications we discuss here. The dynamical matrix for any given model is computed by displacing every atom in the cell by 0.03 Å in three orthogonal directions and calculating the originating forces on all the atoms in the system¹⁰. For a system of thousands atoms the dynamical matrix is very large which, under normal circumstances, causes problems in storing it on disk or in computer memory. Fortunately the dynamical matrix is also very sparse, because in most cases the displacement of a single atom generates significant forces only on its closest neighbors but not in the whole supercell. We extensively exploit this localization of dynamical matrices in our calculations, discarding terms smaller than $10^{-4} \text{eV}\text{Å}^{-2} \text{a.u.m.}^{-1}$, which is a good compromise between accuracy and compactness of the output. Once the sparse dynamical matrix for the system is obtained we use a separate routine to exactly diagonalize the whole matrix and obtain all of the eigenvalues and eigenvectors. Again, for the same reasons as already mentioned above, we do not write out all of the eigenvectors (however, we do keep all their IPRs) but rather only those that exhibit properties we look for: (i) small energy/eigenvalue (less than 200 cm^{-1}) and (ii) relatively high IPR, showing that the vibrational mode we are dealing with is localized.

To create VDOS graphs we employ a Gaussian representation for $\delta(E - E_i)$, where $E_i, i = 1 \dots N$ are the eigenvalues of the dynamical matrix and $N = 3N_{atoms}$. The width of broadening is 20 cm^{-1} for the full scale graphs and 0.1 cm^{-1} for the close-ups of the low-energy region. The vibrational activity colormaps for the “low-energy, high IPR” modes are prepared in same way that has been already described in Sec. II of Ref. 8: the set of individual atomic IPRs is computed and then every atom is assigned a certain color according to its displacement from the equilibrium position.

It is relatively easy to obtain $C(T)$ dependence for the

model if the VDOS information for it is available¹¹:

$$C(T) = 3R \int_0^{E_{max}} \left(\frac{E}{k_B T} \right)^2 \frac{e^{E/k_B T}}{(e^{E/k_B T} - 1)^2} g(E) dE,$$

where VDOS $g(E)$ is normalized to unity. Nevertheless one thing should be treated with caution: the model VDOS one usually has is relevant for a system of *finite* size (i. e. our supercell). Vibrational excitations with wavelengths longer than the size of the supercell cannot be excited in this model and are consequently missing in its VDOS data. In order to receive the precise values for $C(T)$ one should correct VDOS for the *infinite* size of the system. In our case it is done in the following fashion: all the delocalized (acoustic) vibrational modes of energy less than 20 cm^{-1} are cut out and substituted by a weak parabolic tail αE^2 in the routine to compute the VDOS. Parameter α can be obtained from a calculation of the elastic constants of the model¹² but in this investigation we use a more simple approach, fitting α to provide a smooth transition between the low-energy parabolic tail and the rest of VDOS.

III. DISCUSSION OF RESULTS

A. Vibrational properties and localization

We begin this section by presenting the results of our calculations of the low-energy regions¹³ for VDOS and IPR for all the four models introduced above, shown in Fig. 1. For the sake of simplicity we do not present the colormaps for vibrational modes for 4096 atom family of models in this paper, however a set of colormaps for the most interesting localized excitations in these models is available for download over the World Wide Web¹⁴.

From Fig. 1 we can see that the large models for a-Si (both, with and without voids) exhibit quite a complicated vibrational behavior, much more complex than that of smaller 216 atom based families of models, we have studied before^{8,9}. The most important difference here is that a-Si model *without voids* has two localized low-energy modes that are associated with strained regions of silicon network: we have checked bond lengths and bond angles for the atoms in these regions and found that the modes generally localize on atoms with bond angles deviating from the perfect tetrahedral angle by more than 30 degrees.

Consequently, now we have two types of *phonon traps* in our models with voids — the voids themselves and strained regions of the network. Keeping this in mind we can attempt to introduce a rough classification of the localized low-energy modes according to the type of phonon trap they fall into. First, we can see a significant number of vibrational modes in our models with voids that generally show the same kind of localization properties that we have reported earlier⁸: they are exponentially localized with the center of localization positioned to the side

of the void. We classify these excitations as void type modes. Secondly, the modes we might attribute to the *strained network region phonon trap* type in models with voids exhibit a different kind of behavior in comparison to the voidless model. These modes do not localize *exactly* on the strained regions in the supercell; instead they form a string extended between one of these strained regions and the void¹⁵. The possible explanation of this behavior is that these modes can be regarded as a superposition of void type modes and the localized excitations in the model without voids. In our classification we call them mixed type modes. We have to stress once again that the classification we propose is only approximate and is based mostly on the colormaps (i. e. pictures) we get for our models *not* on rigorous mathematical arguments. We must also add that all the low-energy modes, that appear localized in our *finite* models, will be pseudolocalized in an infinite sample¹⁶.

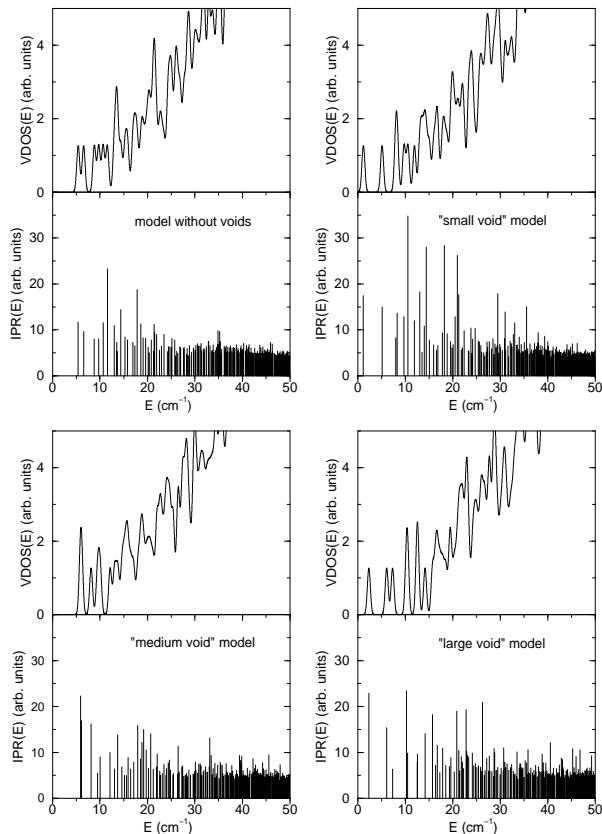


FIG. 1. Low-energy VDOS and IPR snapshots for 4096 atom DTW model without voids (upper left set of panels), 4091 atom “small void” model (upper right), 4069 atom “medium void” model (lower left) and 4008 atom “large void” model (lower right).

We must admit that in our current investigation we were not able to find any simple connection between the size of the void and the energy and type of resulting localized modes. Our data shows that for different models

with voids modes of different types dominate in the low-energy region. In the “small void” model a mode with the highest IPR at 10.58 cm^{-1} is of void type, but the succeeding three modes with high IPR at 14.43 , 18.25 and 20.97 cm^{-1} are of strongly pronounced mixed type. In the “medium void” model, to the contrary, all three low-energy localized modes at 5.89 , 6.12 and 8.13 cm^{-1} are of mixed type. The mode with strong void type behavior is also present but it is shifted to 17.97 cm^{-1} . Finally in the “large void” model modes at 2.34 and 6.10 cm^{-1} are of void type and all the others, including a strongly localized mode at 10.28 cm^{-1} , exhibit mixed type behavior. We *speculate* that the network strain and geometrical peculiarities of any given model play a more important role in shaping the energy and type distribution of its localized vibrational modes than the actual size of the void — at least for the models with voids of comparable sizes, as we have here.

B. Specific heat

In this section we present our results for the calculations of specific heat $C(T)$ for the family of 4096 atom models. The overall temperature dependence for specific heat for all of our models is in good agreement with Dulong and Petit’s law at high temperatures and Debye’s law at low temperatures; our calculation also produces approximately the correct Debye temperature for a-Si. For the room temperature (300K) we receive practically the same value for specific heat for all of our models: $19.7 \text{ JK}^{-1} \text{ mol}^{-1}$.

In the left panel of Fig. 2 the $C(T)/T^3$ low-temperature dependence for our models is presented. The most striking feature in this graph is the presence of sharp peaks at $T < 3\text{K}$ in the curves for the models *containing voids*. The model without voids *does not* have this peak, although it does demonstrate the presence of the well known excess specific heat bulge, the position and height of which are in qualitative agreement with experiment¹⁷ as well as with recent computational results of Feldman, Allen and Bickham¹⁶. All of our models with voids also have the excess specific heat bulges at approximately the same position, but comparing to the low-temperature peaks their intensities are about an order of magnitude smaller. We were not able to find any experimental data for specific heat measurements in a-Si at temperatures below 2K , but in order to make some general comparison to experiment for these new low-temperature features we obtain (which should be generic for *any* disordered system containing voids), we provide the experimental curve for vitreous silica¹⁸ in our graph.

Unlike the previous void size vs. energy situation, we can find a clear connection between the presence of low-energy localized modes in vibrational spectrum of the model and the height (or even absence) of the low-temperature peak in its $C(T)/T^3$ graph. For the “small

void” model we have a localized mode at 1.19 cm^{-1} (here and below, see Fig. 1) — the lowest energy at which we can see localized excitations in all our models — and the highest peak in $C(T)/T^3$ dependence. The “large void” model has its lowest energy localized excitation at 2.34 cm^{-1} and the peak of smaller height comparing to the previous model. The “medium void” model has two localized states but only at approximately 6 cm^{-1} and peak that is even less pronounced than in case of the first two models. Finally the model without voids has no localized states with energy lower than 11 cm^{-1} and *no low-temperature peak whatsoever*.

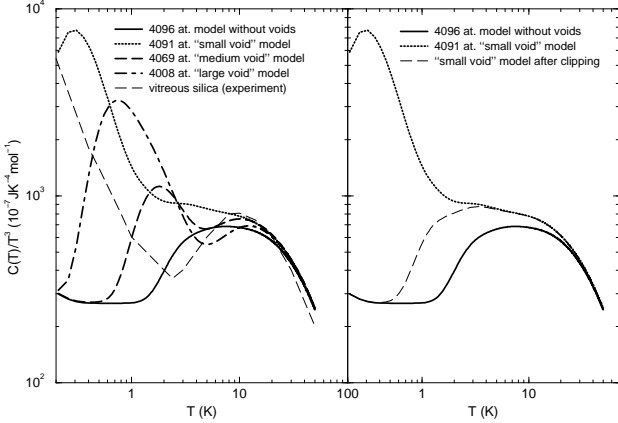


FIG. 2. Left panel: the low-temperature $C(T)/T^3$ dependence for the DTW models with and without voids. The experimental curve for vitreous silica is taken from Ref. 18. Right panel: the curves for 4091 atom “small void” model before and after clipping of the lowest energy localized mode eigenvalue. Curve for the model without voids is also shown for reference.

In order to investigate this connection in more detail we have performed a simple numerical experiment, which results are shown in the right panel of Fig. 2. We have clipped the eigenvalue at 1.19 cm^{-1} from the eigenvalue set for the “small void” model and recalculated its VDOS and $C(T)$ receiving no low-temperature peak in $C(T)/T^3$ graph, much like in the situation with the model without voids. In our opinion these results provide enough evidence to attribute the existence of low-temperature ($T < 3 \text{ K}$) peak in $C(T)/T^3$ dependence for the model to the presence of localized low-energy ($E \sim 1 - 6 \text{ cm}^{-1}$) vibrational excitations — in our case produced by voids — in its spectrum.

Finally we must note that the localized vibrational excitations we see, although having rather low energies, are *not* tunneling states¹⁸, that are nonharmonic by nature and can not be obtained in harmonic approximation calculation. We do not claim that the whole tunneling states theory is incorrect, we rather propose an alternative mechanism that explains the same experimental data. It seems that *any* mechanism that creates additional density of vibrational states (be this tunneling states or low-energy localized “void” vibrations in porous

materials) at very low energies will produce the same effect on low-temperature specific heat behavior. In order to find out which mechanism of the two mentioned above *actually works* in real material, an experimental investigation of low-temperature thermal properties and *simultaneously* geometrical quality (i.e. presence of defects, voids, strained regions) of this material should be carried out. The works of X. Liu *et al.*^{19,20} or Coeck and Laermans²¹ for amorphous silicon can be regarded as the closest examples here.

IV. CONCLUSIONS

We have studied vibrational and thermodynamical properties of 4096 atom DTW model for amorphous silicon and the family of models with voids based on it, employing Bazant-Kaxiras environment-dependent interatomic potential and empirical MD technique. We have found that the models with voids possess a complex spectrum of localized low-energy excitations that can be *roughly* divided into two groups — void and mixed type modes — according to their localization patterns. Our calculations show that there is no simple connection between the size of the void and the energy and type of its localized modes. It is most probable that not only the size of the void but also its local geometrical environment as well as strain distribution in the neighboring regions of the network play a paramount role in shaping the low-energy vibrational spectrum of the system. We have constructed specific heat $C(T)$ plots for our models, that appear to be in good agreement with experiment. We have also plotted out our models’ $C(T)/T^3$ dependences for the low-temperature region, which seem to be in adequate agreement with experimental and other computational results for $T > 3 \text{ K}$ (the excess specific heat bulge) and predict new interesting features, undoubtedly connected with vibrational properties of voids present in the system, at lower temperatures. We must stress that our results are correct for model materials with a *uniform* distribution of voids of *one and the same size*, which is of course impossible to produce in real material. Nevertheless, employing our model data we can predict that in real material the localized low-energy vibrational states, connected to voids of different sizes, will fill out a band which will alter the parabolic VDOS tail properties at small energies and consequently manifest itself by changing the specific heat $C(T)/T^3$ dependence.

ACKNOWLEDGMENTS

This work was supported by NSF under grant number DMR 96-04921 and DMR 96-18789. We thank Prof. Normand Mousseau for many helpful discussions.

- ¹ B. R. Djordjevic, M. F. Thorpe and F. Wooten, Phys. Rev. B **52**, 5685 (1995).
- ² F. Wooten, K. Winer and D. Weaire, Phys. Rev. Lett. **54**, 1392 (1985).
- ³ See, for example, R. Biswas, A. M. Bouchard, W. A. Kamitakahara, G. S. Grest and C. M. Soukoulis, Phys. Rev. Lett. **60**, 2280 (1988).
- ⁴ M. Z. Bazant and E. Kaxiras, Phys. Rev. Lett. **77**, 4370 (1996);
- ⁵ M. Z. Bazant, E. Kaxiras, J. F. Justo, Phys. Rev. B **56**, 8542 (1997);
- ⁶ J. F. Justo, M. Z. Bazant, E. Kaxiras, V. V. Bulatov, and S. Yip, Phys. Rev. B **58**, 2539 (1998).
- ⁷ F. H. Stillinger and T. A. Weber, Phys. Rev. B **31**, 5262 (1985).
- ⁸ S. M. Nakhmanson and D. A. Drabold, Phys. Rev. B **58**, 15325 (1998).
- ⁹ S. M. Nakhmanson and D. A. Drabold, J. Noncryst. Solids (to be published).
- ¹⁰ O. F. Sankey and G. B. Adams (unpublished).
- ¹¹ See, for example, Sec. IV of A. A. Maradudin *et. al.*, *Theory of Lattice Dynamics in the Harmonic Approximation* (Academic Press, New York and London, 1971).
- ¹² J. L. Feldman (private communication); for the elastic constants calculation details, see J. L. Feldman and J. Q. Broughton, F. Wooten, Phys. Rev. B **43**, 2152 (1991), and references therein.
- ¹³ For full scale VDOS and comparison to experiment see Ref. 9.
- ¹⁴ <http://www.phy.ohiou.edu/~nakhmans/Professional/Colormaps/colormaps.htm>
- ¹⁵ In J. J. Dong and D. A. Drabold, Phys. Rev. Lett. **80**, 1928 (1998) the similar localization behavior is observed for the *electronic* states in the band-gap region for DTW model for a-Si.
- ¹⁶ J. L. Feldman, P. B. Allen, S. R. Bickham, Phys. Rev. B **59**, 3551 (1999).
- ¹⁷ M. Mertig, G. Pompe and E. Hegenbarth, Solid State Commun. **49**, 369 (1984).
- ¹⁸ W. A. Phillips, Rep. Prog. Phys. **50**, 1657 (1987), and references therein.
- ¹⁹ X. Liu, B. E. White, Jr., R. O. Pohl, E. Iwanizcko, K. M. Jones, A. H. Mahan, B. N. Nelson, R. S. Crandall and S. Veprek, Phys. Rev. Lett. **78**, 4418 (1997).
- ²⁰ X. Liu, P. D. Vu and R. O. Pohl, F. Schiettekatte and S. Roorda, Phys. Rev. Lett. **81**, 3171 (1998).
- ²¹ M. Coeck, C. Laermans, Phys. Rev. B **58**, 6708 (1998).